Computers in Biology and Medicine 106 (2019) 150–156

Contents lists available at ScienceDirect

Computers in Biology and Medicine

journal homepage: www.elsevier.com/locate/compbiomed

Color masking improves classification of celiac disease in videocapsule endoscopy images

Edward J. Ciaccio[a,*], Suzanne K. Lewis[a], Govind Bhagat[a,b], Peter H. Green[a]

[a] Department of Medicine – Celiac Disease Center, Columbia University College of Physicians and Surgeons, New York, NY, USA
[b] Department of Pathology and Cell Biology, Columbia University College of Physicians and Surgeons, New York, NY, USA

ARTICLE INFO

Keywords:
Celiac disease
Masking
Mucosa
Videocapsule
Villous atrophy

ABSTRACT

Background: Videocapsule endoscopy images are useful to detect pathologic alterations, including villous atrophy, in the small intestinal mucosa, which is helpful for diagnosing celiac disease. In prior work, quantitative videocapsule analysis was found useful to classify celiac versus control images. However, the effect of dark/extraneous substances on classification efficacy requires remediation.

Method: For quantitative analysis, data from the Medtronic SB2 and SB3 systems were pooled. Videocapsule images of the distal duodenum/proximal jejunum were acquired from 13 celiac and 13 control patients. Dark regions, extraneous fluids, and air bubbles were mostly removed by utilizing color masking. Two different red-green-blue (RGB) color masks were constructed from 20 to 30 reference pixels obtained from mucosal and from extraneous regions. Each image pixel was accepted or rejected for subsequent analysis based on whether its distance was closest to a mucosal or to an extraneous reference in RGB space. Four images were then randomly selected from each videoclip for processing (52 images from each group). After masking, celiac versus control images were plotted in a three-space consisting of mean and standard deviation in pixel brightness, and surface area remaining after masking. A linear discriminant function was used for classification. The paradigm was repeated with a second random data set for validation.

Results: Masking improved classification of celiac versus control images to nearly 80% accuracy as compared to 70–77% without masking. Celiac disease patients tended to have lesser mean pixel brightness and greater variability in brightness, in accord with prior work, and more masking was needed to remove extraneous features.

Conclusions: Color masking is useful to remove dim/extraneous features from videocapsule images and it results in improved classification/assessment to distinguish celiac with villous atrophy from control videocapsule image. This can be helpful to detect and map regions of pathology, to screen for celiac disease, and to determine the efficacy of a gluten free diet.

1. Introduction

Celiac disease affects approximately 1% of the population worldwide [1]. Individuals with this autoimmune disease mount an immune response to dietary gluten [2]. Gluten is found in wheat, rye, and barley, which are staples in much of the world. In celiac patients, consuming these grains can lead to damage of the small intestinal mucosa [3], as well as an increased risk of extra-gastrointestinal disorders [4], including effects on the cardiovascular [5] and neurologic systems. Currently, the main treatment is abstaining from consumption of gluten-containing grains [6]. Diagnosis of celiac disease is difficult because the symptoms can vary substantially from one patient to the next. There is often, though not always, pathology of the small intestinal mucosa in the form of villous atrophy [7], which is visualized as fissuring, mottled appearance (from clumping of the villi), and scalloping of the mucosal folds on endoscopy. The extent of these changes also varies from one patient to the next. For definitive diagnosis, biopsy of the small intestinal mucosa is performed during standard endoscopy [8], and serology is used to determine reaction to autoantibodies. However, villous atrophy is often patchy [9], and it may be difficult to select suitable areas of the small bowel pathology to biopsy, which is required for correct diagnosis. To confirm the diagnosis, patients should recover from symptoms on a gluten-free diet [10]. Yet, some patients are refractory to treatment, and may only show partial recovery of small bowel histology and symptoms on the diet, if at all [11]. Thus, the need for more quantitative means to detect

* Corresponding author. Columbia University, PH 9-934, 180 Fort Washington Avenue, New York, NY, 10032, USA.
E-mail address: ciaccio@columbia.edu (E.J. Ciaccio).

https://doi.org/10.1016/j.compbiomed.2018.12.011
Received 2 August 2018; Received in revised form 10 December 2018; Accepted 18 December 2018

pathology in endoscopy images and to monitor patient status.

In prior work, we described a variety of methods to detect the presence of villous atrophy in celiac disease patients undergoing videocapsule endoscopy [12–17]. Construction of basis images, which are derived from eigenanalysis and represent salient features contained in a set of videoclip images, have been found useful to classify celiac versus control images with nonlinear discriminant functions [15]. Three-dimensional modeling using shape-from-shading principles can be implemented to form an approximation of the mucosal architecture, which can then be classified using syntactic (i.e., shape-based) techniques to define the presence and types of mucosal protrusions [16]. Celiac patients tend to have protrusions with greater length and width dimensions as compared to controls, which may be due to clumping of the villi, seen as a mosaic (cobblestone or mottled) macro-architectural pattern in videoclip images. Motility of the small intestinal lumen, which can be quantitated based upon the centroid location of the dimmest pixel regions, has been found to be reduced in celiacs as compared with controls, particularly in areas of suspected pathology along the small intestine [13]. Spectral analysis may also be assistive as an estimate of motility [12]. Pixel brightness and variation were found useful to quantitate textural properties of the intestinal mucosa in celiac disease [17]. Automata-based polling of many methods (i.e., majority vote technique) can also indicate regions of mucosal villous atrophy in celiac disease [14].

The above-described methods, however, may sometimes be unwieldy due to the complexity of the technical procedures, and some also require *a priori* information as well as the creation of nonlinear discriminant functions. If a technique were available that was easy to use and did not require the construction of special linear or nonlinear discriminant functions for analysis and classification of pathology in the celiac patient videocapsule data at hand, it could go a long way toward simplifying the analysis of these data for purposes of diagnosis and monitoring. Herein, a technique is described for this application, which imparts color masking to remove extraneous materials, thereby improving accuracy in detecting celiac versus control images from randomly selected data.

2. Method

The PillCam SB2 and SB3 systems (Given Imaging/Medtronic, Parsippany, NJ) were used to acquire videocapsule data for this study [18]. The PillCam SB2 operates with a fixed frame rate for imaging of 2 photos per second [19]. The PillCam SB3 operates with variable frame rate technology of from 2 to 6 photos per second [20]. Data were acquired in the small intestine from a total of 13 patients with untreated celiac disease and villous atrophy, prior to the start of a gluten-free diet, and from 13 control patients lacking villous atrophy. Videoclips consisted of 100, 200, or 1000 image frames each from the duodenal bulb, distal duodenum, proximal jejunum, and ileum in each patient. Videoclips of the distal duodenum/proximal jejunum, where pathology is most likely to occur, were used for further analysis. Table 1 provides additional information. The videocapsule data were obtained from nine celiac patients and eight control patients using the PillCam SB2 system. Data was also obtained from the same locations of four celiac patients and five control patients using the PillCam SB3 system. The system for obtaining data consisted of a swallowable capsule (i.e., PillCam) that included a camera, lighting system, and internal electronics. Data were sent in real time by radiofrequency to a recorder strapped to the patient. The data could be monitored in real time, and was also archived for subsequent analysis. Each patient swallowed the PillCam in the early morning with water, following a midnight fast. The PillCam passed harmlessly through the digestive system in each patient, requiring approximately 8 h for passage. The data from the console was then ported without patient identifiers for subsequent analysis on a dedicated workstation. This work was approved by the Columbia University IRB.

Table 1
Patient videocapsule data.

SB2-cel	SB2-con	SB2-tot	SB3-cel	SB3-con	SB3-tot	Cel-tot	Con-tot
9	8	17	4	5	9	13	13

cel = celiac, con = control, tot = total.

The quantitative analysis protocol consisted of comparing and classifying celiac versus control images, as a means of identifying the presence of villous atrophy and other pathology in the celiac patients. It was supposed, to a first approximation for the study, that all celiac videocapsule image areas contained small intestinal mucosa with villous atrophy, although this may only be partially correct, as the pathologic regions tend to be patchy in location. In prior work, dark areas which appear with lower brightness resolution, as well as extraneous features, including the presence of opaque fluids, air bubbles, and other substances, were included in the subsequent analysis [12–17]. In these studies, it was supposed that the undesirable features acted as random noise, which could however reduce the significance of the difference in the classification of celiac versus control images. In the current study, a means was devised to mask dim areas and extraneous substances present in the videocapsule images, to determine whether this would increase significance in distinguishing images obtained from celiac patients versus controls, and whether it would enable a fixed linear discriminant function, rather than variable and/or nonlinear discriminant functions, to be used for discernment of celiac versus control images.

To remove extraneous substances from the videoclip images prior to processing, color information was quantified, as has been done in prior studies [21,22]. Two color masks were created. An exemplar videocapsule image from one celiac and one control patient (acquired with the SB2 PillCam) were used for this purpose. One mask (i.e., mask A) was created by manually selecting and defining 30 pixels as being representative of the small intestinal mucosa and 30 pixels as being representative of dim/extraneous features. The second mask (mask B) was created using a subset of only 20 of the 30 mucosal reference points and 20 of the 30 extraneous reference points from mask A. Each of the reference pixels was defined by its magnitude in red-blue-green (RGB) color space. Dim/extraneous feature pixels were then identified in data obtained from the patients, described in Table 1, as follows. Four images were selected at random from each videoclip. For each image, all pixels were analyzed. The dimensions of each image after storing in the ppm format, for ease of analysis, and after cropping to remove lettering and borders, was 1500×1500 pixels $\approx 2\,\mathrm{E}\,6$ pixels in total. Although the original image resolution was 576×576 pixels for the SB2 system, upsampling was done during the masking process, which did not add information, but made the process easier to implement. The Euclidean distance was then calculated in the RGB space, being the distance in three color dimensions from pixel being analyzed in the input image, to each of the 60 defining points for Mask A, and to each of the 40 defining points for Mask B. The pixel being analyzed was determined to belong to the mucosal substrate if it was closest to a mucosal reference point, and it was determined as being an dim/extraneous feature if it was closest to a dim/extraneous reference point. Pixels determined to be dim/extraneous points were not included in the subsequent, processing stage of the analysis.

During the processing stage, the remaining image portions after color masking for removal of dim/extraneous features were analyzed. In this stage, each image was described by its mean pixel brightness, by the standard deviation (i.e., variation) in pixel brightness, and by the total surface area (number of pixels) remaining in the image after masking. The means/standard deviations in pixel brightness were computed for each of the colors red, green, and blue, and three scatterplots, for the three colors, were drawn for mask A and three for mask B (six graphs in all). The axes of the first scatterplot consisted of mean

red brightness value, standard deviation in red brightness value, and number of pixels remaining in each image after masking (mask A). The axes of the second and third scatterplots were similar to the first, except that mean and standard deviation values of green and blue color, respectively, were used for the first two axes (mask A). The same graphs were created using mask B. The points of the six scatterplots were thus representative of the patient data described in Table 1, with four images used from each videoclip. Thus for the 26 patient data of Table 1, there were 26 × 4 = 104 points in each scatterplot; 52 of these points were from the 13 celiac patients (denoted as solid circles) and 52 were from the 13 control patients (denoted as hollow circles). The scatterplots were rotated to a standard view so that differences could be readily visualized (horizontal 153°, vertical 42°, perspective 20°). The three-space of each scatterplot was then projected into two dimensions, and a linear discriminant function (LDF) was used to best separate the scatterpoints of celiac versus control data for classification, in each of the six graphs. Thereafter, a second data set was obtained (i.e., four additional images selected at random from each of the 26 videoclips). New scatterplots were created from these data, with the same LDFs as prior being used to classify it. LDFs were created to classify the data without any masking, as a comparison to determine the efficacy of the masking process. Finally, classification accuracy separately using PillCam SB2 versus PillCam SB3 was also determined.

3. Results

3.1. Summary statistics

Classification Results after forming the LDFs, for both mask A and mask B, are provided in Table 2. The average classification accuracy in RGB color space for data set 1 was 78.5 ± 10.5, and for data set 2 it was 78.8 ± 15.1. There were also similar accuracies for mask A and mask B, celiacs and controls, for first versus second data set (bottom row in Tables 2A and 2B). Thus the same LDFs used for a second set of data had similar accuracy in separating celiac from control images. Differences in accuracies for mask A versus B can be attributed to differences in the LDFs developed for each.

In Table 3, classification accuracies are shown when no mask was used on the videoclip images (extraneous features not removed). The average classification accuracy in RGB space for the initial data set was 76.9 ± 8.8% (celiacs and controls combined). The average accuracy for the second data set was 70.5 ± 22.2% (celiacs and controls combined). These accuracies in classification were lower as compared with the means for masked data (Table 2). Hence, color masking was useful to improve classification Results.

In Table 4, Results of classification for PillCam SB2 versus SB3 data are shown for the first data set. The average accuracy for classification of the PillCam SB2 data was over 80% while the average accuracy for PillCam SB3 data was about 70% (mask A and mask B). The lower accuracy for SB3 data (Table 4) may have resulted from the larger number of SB2 as compared with SB3 videoclips (Table 1: 17 versus 9), thus biasing the LDFs toward the SB2 data characteristics. However, the accuracy of SB3 data, nearly 70%, was still substantially higher than would be attributed to random chance (50%).

In Fig. 1 the data are shown for red color, mask A, data set 2. Solid circles represent celiac videoclips while hollow circles represent controls. Celiac points tend to be the lowest in the distribution (lesser values designate that the mask removed more extraneous features in those images). Many of the control images (represented by hollow circles) tend to reside at higher values of mean red pixel intensity, whereas celiac images (solid circles) often reside at lesser mean red pixel values. Thus, control images in the data set tended to be brighter in red color value as compared to celiacs. Many celiac images (solid circles) have a high standard deviation in red intensity as compared with control images (hollow circles). Therefore, many of the celiac images tend to be more variable in brightness as compared with controls. Although not shown for brevity, similar Results as in Fig. 1 were obtained for green and blue color values. Fig. 2 shows similar results as Fig. 1, except that mask B was utilized. Similar results for data set 1.

In Fig. 3, red, green, and blue scatterplots are presented for the data when no preprocessing was performed (masks not used). The scatterplots show that all of the images for both celiacs and controls reside at the plateau level of approximately 2 E 6 pixels, which is the image surface area in total number of pixels when no mask is used (full image). Slight deviations from this value occur because each image was cropped manually to remove extrinsic wording and borders.

Comparative examples of color masking are provided in Fig. 4. In panels A–C, the Results from a control patient are shown. Panel A is

Table 2A
Combined SB2 and SB3, with masks A and B - Data Set 1 (percent accuracy).

A-con	A-cel	B-con	B-cel	Color
78.8	78.8	67.3	86.5	Red
82.7	71.2	63.4	90.4	Green
94.2	73.1	65.4	90.4	Blue
85.2 ± 8.0	74.4 ± 4.0	65.4 ± 2.0	89.1 ± 2.3	MN ± SD

A = mask A, B = mask B, cel = celiac, con = control, tot = total.
Mean, Data1: 78.5 ± 10.5.

Table 2B
Combined SB2 and SB3, with masks A and B - Data Set 2 (percent accuracy).

A-con	A-cel	B-con	B-cel	Color
78.8	82.7	75.0	82.7	Red
86.5	76.9	51.9	100.0	Green
98.1	63.5	57.7	92.3	Blue
87.8 ± 9.7	74.4 ± 9.8	61.5 ± 12.0	91.7 ± 8.7	MN ± SD

A = mask A, B = mask B, cel = celiac, con = control, tot = total.
Mean, Data2: 78.8 ± 15.1.

Table 3
Combined SB2 and SB3, no masking (percent accuracy). Data Set 1 (Data1) Data Set 2 (Data2). Mean, Data1: 76.9 ± 8.8. Mean, Data2: 72.1 ± 10.9.

Control - Data1	Celiac - Data1	Control - Data2	Celiac - Data2	Color
65.4	82.7	65.4	69.2	Red
67.3	82.7	69.2	78.8	Green
86.5	76.9	90.4	59.6	Blue
73.1 ± 11.7	80.8 ± 3.3	75.0 ± 13.5	69.2 ± 9.6	MN ± SD

Table 4A
SB2 masking (percent accuracy).

A-con	A-cel	B-con	B-cel	Color
78.1	86.1	68.8	97.2	Red
93.8	75.0	65.6	94.4	Green
100.0	75.0	68.8	91.7	Blue
90.6 ± 11.3	78.7 ± 6.4	67.7 ± 1.8	94.4 ± 2.8	MN ± SD

A = mask A, B = mask B, cel = celiac, con = control, tot = total.
Mean, mask A: 84.7 ± 10.5. Mean, mask B: 81.1 ± 14.8.

Table 4B
SB3, masking (percent accuracy).

A-con	A-cel	B-con	B-cel	Color
70.0	75.0	60.0	75.0	Red
70.0	75.0	80.0	75.0	Green
95.0	50.0	35.0	81.3	Blue
78.3 ± 14.4	66.7 ± 14.4	58.3 ± 22.5	77.1 ± 3.6	MN ± SD

A = mask A, B = mask B, cel = celiac, con = control, tot = total.
Mean, mask A: 72.5 ± 14.4. Mean, mask B: 67.7 ± 17.7.

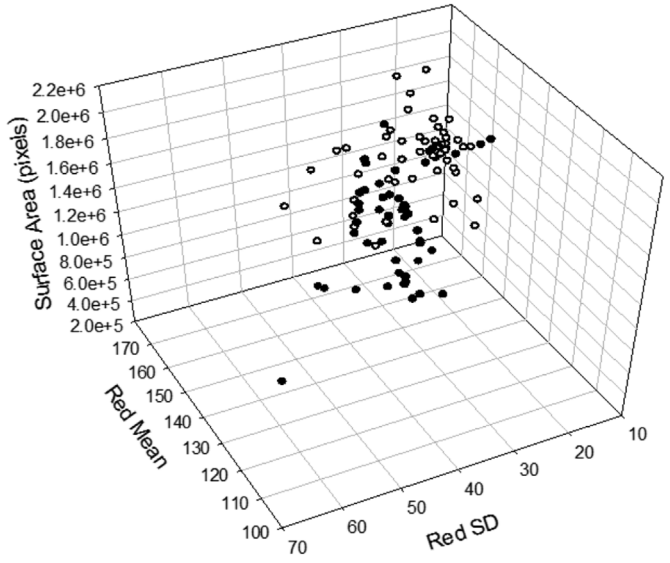

Fig. 1. Red color, data set 2, mask A. Scatterplot from celiac videocapsule data (solid circles) and controls (hollow circles). A. Celiac points tend to have lesser surface area after masking (greater reduction in size due to color mask), lesser mean pixel intensity and therefore dimmer on average, and greater standard deviation or variance (less uniform in brightness), as compared with control data.

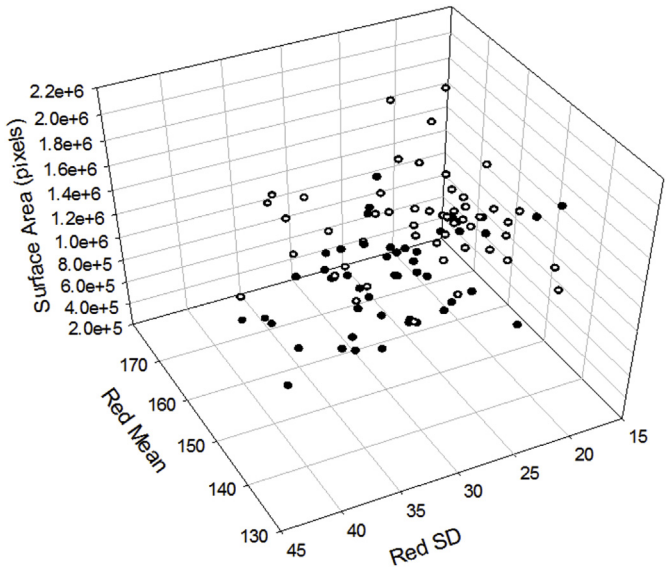

Fig. 2. Red color, data set 2, mask B. As for mask A shown in Fig. 1, celiac videocapsule images, represented by solid circles, tend to have slightly less surface area after masking, many tend to be dimmer images in the sense of having lesser mean red intensity value, and often the standard deviation in red intensity value is greater, as compared with controls (hollow circles). Similar Results were obtained for green and blue values in celiacs versus controls, mask B and for data set 1.

non-masked, panel B is the result using mask A, and panel C is the result using mask B. Mask B removed more of the original image as compared with mask A, even though it is defined with 20 mucosal and 20 dim/extraneous reference points instead of 30 and 30 as in mask A. Many dim areas are treated as extraneous features and are identified and removed by both masks, as intended. Some, but not all, of the yellow opaque fluid area noted in panel A is removed in panels B and C. In panels D–F, images from a celiac patient are shown (non-masked, Mask A, and Mask B, respectively). Dim areas and extraneous features are removed here as well. Mask A also removes the yellow opaque fluid areas at lower left (panel E) better than mask B (panel F). However, mask B removes more of the darker regions (top of image) as compared with mask A. Thus, the number of reference points does not necessarily correlate to the degree of dim/extraneous feature removal. Depending upon the mucosal versus dim/extraneous point references, the degree of masking may increase or decrease as more references points are utilized. A mottled appearance caused by pathology is evident in the celiac images (panels D–F).

4. Discussion

4.1. Summary

In this study, videocapsule images from untreated celiac patients and from control patients were examined. The celiac patient data were acquired prior to commencement of a gluten-free diet, the main and lifelong treatment for the disease. The underlying hypothesis was that in celiac disease, villous atrophy, which is evident as fissuring, clumping of villi, which results in a mottled appearance, and scalloping of mucosal folds, affect the structural makeup that is viewable in the macroscopic images obtained by the PillCam system. For purposes of classification of celiac versus control images, it was supposed that such differences in features will be manifested as statistical differences that are evident by quantitation of the videocapsule images. The videoclips were first analyzed in RGB color space as a preprocessing step. To remove extraneous features, a three-dimensional color mask was used, consisting of representative and labeled points from the small intestinal mucosa, or from dim areas limited in resolution/extraneous features such as opaque fluids and air bubbles. During preprocessing, all pixels in each image were assessed for Euclidean distance to these reference data points. The reference point with shortest distance to each pixel's colormap was used to define the pixel as being either mucosal substrate or dim lumen/extraneous matter. Only pixels labeled as being mucosal in each image were further analyzed. From this remaining pixular area, the mean and standard deviation in brightness (separately for all three colors) and the surface area (pixel number), were computed. These three variables are not dependent upon the shape of the image after masking. Scatterplots were then made of the trivariables for each of the three colors. Since two different sets of mask reference points were tested (resulting in mask A and mask B), six scatterplots were constructed in total.

After processing, the orientation of the scatterplots was normalized for viewing, and these were projected onto two-dimensional surfaces. A linear discriminant function was constructed to best separate celiac from control data for each of the scatterplots. The classification accuracy to distinguish celiac from control image points was determined. Using the same LDFs, a second set of randomly selected data from the same patient data sets (Table 1) was analyzed and the classification performance was recorded. A classification accuracy of nearly 80% was found for both sets of data (Table 2). The classification accuracy was improved when using either of the color masks to remove dim areas and extraneous matter as compared with not using a color mask (Table 3) and therefore not removing dim/extraneous regions. Lastly, the data were separated as to whether they were acquired with the PillCam SB2 or SB3 system, and then reclassified (Table 4). The PillCam SB2 data, from which 17 patient videoclips were acquired, was found to be more accurately classified as compared to PillCam SB3, with 9 videoclips. This may be attributable to the fact that more samples from SB2 were included in the analysis and used to form the LDFs (Table 1).

4.2. Algorithm discussion

Videocapsule endoscopy has been previously shown to potentially be assistive for celiac disease diagnosis [23,24]. For preprocessing of videocapsule data, in the current study, a pixel was either selected (mucosal) or rejected (dim/extraneous) based upon the closest distance

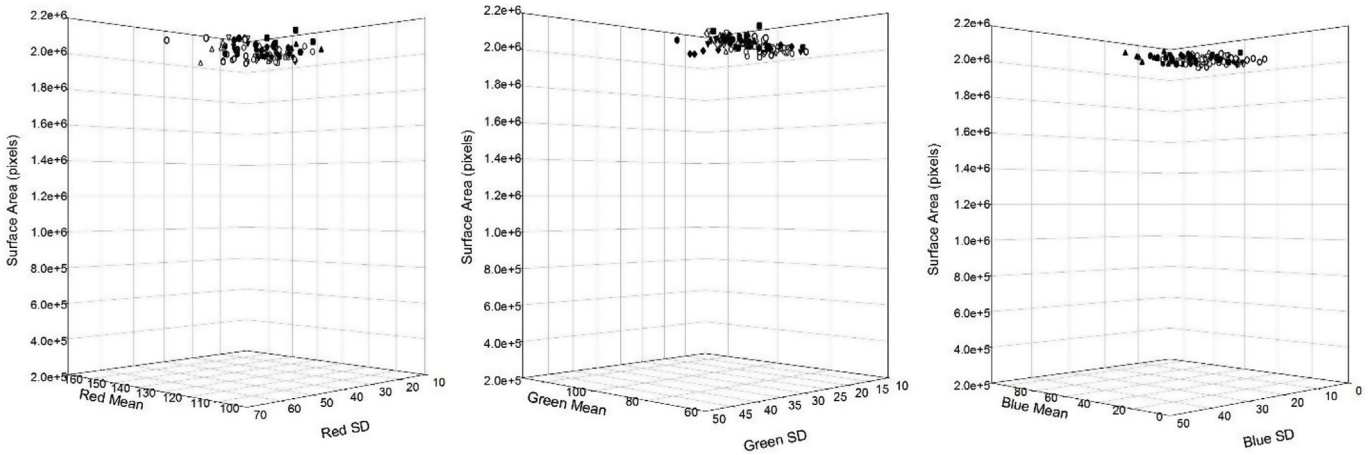

Fig. 3. Distribution of data when no color mask filtering is done. The data is projected to show that both celiac (solid circles) and control (hollow circles) cluster at a surface area of 2.2 E6 in value, i.e., the entire image, of surface area 2.2 E6 pixels, is left undisturbed. Shown for red, green, and blue color values. This means that the entire image (all image pixels) was used for processing, i.e., no masking was utilized.

in RGB space to a set of reference points. This method supposes that the color content of all of the reference points only represents a single class (mucosal versus extraneous) and never represents the other class. However, it is likely that sometimes a particular RGB color can be representative of either class. For example, in Fig. 4B and C, dim regions and extraneous features remain to some extent after masking. This might be remedied by one of two means. Firstly, employing more reference pixels to define mucosal and extraneous regions could be helpful to better characterize each region. However, this will not be assistive when a particular color is evident in both mucosal and extraneous image regions. Secondly, a majority vote method could be implemented. One example of this would be to measure the distances from a particular pixel to all reference points. Then to compute the mean (or median) distance from said pixel to all mucosal reference points and the mean (median) distance from said pixel to all dim/extraneous reference points in the three color dimensions. The lower mean (or median) distance would win, and the pixel would thereby be classified. Similarly, the top 5, 10, or x closest distances between pixel and all reference points could be determined. The pixel would be selected as mucosal or extraneous according to how many reference points of each was in the top 5, 10, or x shortest distances. A computer aided detection system (CAD), which has been shown to be efficacious for celiac disease classification using the DWT algorithm [25], may be utilized to further improve the color masking process.

During image processing, the three-space used to plot the scatterpoints were the mean and standard deviation in pixel brightness for each color, and the surface area remaining after preprocessing by color masking. The statistical measures of mean and standard deviation are readily calculated, they can be rapidly computed, and they do not require a contiguous surface area for calculation. Regardless of the image shape after masking for removal of dim/extraneous content, these two statistical measures are calculable. The Results showed that brighter image scene (higher mean value) and lesser variability in texture (reduced standard deviation) tend to be more characteristic of control videocapsule data lacking villous atrophy and lacking other pathologic features (Figs. 1 and 2). Whereas, there is a tendency for darker image features, and more variable textural content, in the celiac images. This contributed to the efficacy of the technique for classification of celiac versus control images, and is in accord with prior work performed with grayscale images [12–17]. It suggests that pathologic regions in

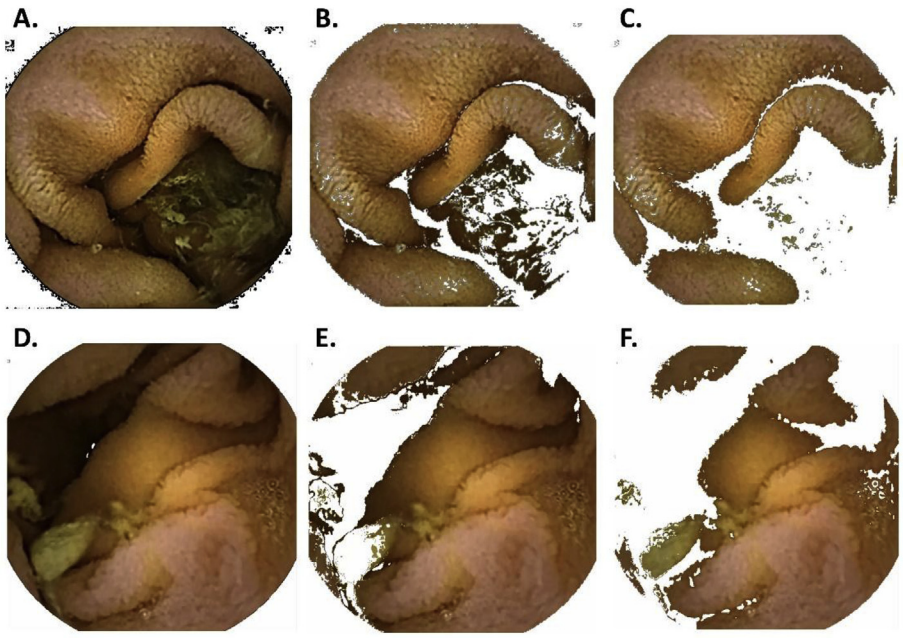

Fig. 4. Examples of tricolor videocapsule images. A-C. Control patient data. Panel A shows the image sans masking, while panel B is the image filtered using mask A, and panel C is the image filtered with mask B. D-F. Celiac patient data. Panel A shows the image sans masking, while panel B is the image filtered with mask A, and panel C is the image filtered with mask B. In both cases, masking removes dark regions/extraneous features to varying extents. A mottled appearance is evident in the celiac images, which is characteristic of areas with villous atrophy.

videocapsule images are darker and more variable as compared with normal small intestinal mucosa, which would be more uniform and brighter. Thus, color mapping tends to well preserve image characteristics and provides additional quantitative representation.

4.3. Limitations and future work

As a first approximation, it was supposed that celiac images would all contain villous atrophy or other pathology, which would be utilizable to distinguish them from control images. However, some celiac images will actually have an entirely normal appearance at the level of the videocapsule imagery, in which case they should not be separable from controls by automated means, one reason for a reduction in accuracy. The only way to surmount this dilemma would be to biopsy the area of each videocapsule image, and include only celiac images with verified villous atrophy in the celiac cohort, which is presently impracticable. The number of videoclips utilized in the study were also limited. Over time, more patient data will be used to expand the study. Although classification accuracy was reduced using SB3 (Table 4), it is likely that the accuracy will improve as more patient data from this system are included for subsequent analysis. Once LDFs have been developed over a large N of patient data input, there will likely be less need for their recalculation in subsequent patient studies. It might then be possible to analyze incoming videocapsule data automatically in real time without *a priori* information, using LDFs calculated from prior data, the subject of future work.

Extraneous substances limit the utility of videocapsule endoscopy [26,27]. The color masks for rejecting darker/extraneous features in the current study were based upon a limited set of reference points. Application of additional reference points in future work, and in so doing to construct additional masks, may be useful for more accurate removal of image areas not relevant to the analysis. However, there is likely some overlap in the color mapping of mucosal versus dim/extraneous features, as described above. Any such overlap would require additional sophisticated methods to remedy. One such approach would be to use spatial context. For example, pixels classified as dark, surrounded by many other pixels classified as dark (i.e. based upon spatial context), would be suggested as belonging to dim image regions that should not be used for further processing. However, pixels that are dark, which belong to fissured regions as defined by some syntax, i.e., having some bright and some dark pixels according to the shape of the fissure, would be classified as intestinal mucosa (they are regions of pathology in celiac patients and relevant for further processing). Dim pixels belonging to fissured regions could also be discerned based upon spatial context, by supposing that if proximate surrounding pixels are mostly mucosa according to the colormap, such dark pixels should also be classified as mucosa and not filtered out by the mask. A syntax could be carefully constructed for such purposes. The effect of implementing context-based methodology should be evaluated in future work.

Finally, only a single viewpoint was used to project the three-space into two dimensions for constructing LDFs and classifying celiac versus control images. The orientation of the scatterplots for this purpose was not optimized. Hence, other scatterplot orientations might be useful to improve the spread of celiac versus control points in the graphs. This could result in some improvement in accuracy, and should be optimized with a larger patient number N, the subject of additional research.

5. Conclusions

Herein, methodology was described to eliminate dark/extraneous regions from videocapsule images, as a preprocessing stage prior to image representation and classification. It was evident that such methodology, both using mask A and mask B, are useful to improve representation as well as classification performance (see Results section). The data were represented in a three-space using color brightness, standard deviation, and surface area of the remaining image after masking, as the three variables for analysis. This was done for each of the tricolor data (red-green-blue). It was evident that the mean (image feature brightness) and standard deviation (variability, or uniformity, in image features) were both useful for differentiating celiac versus control videocapsule data (Tables 2–4). Celiac data also tended to have more dim/extraneous features that were masked. The spread in the scatterplot distributions - with celiac data tending to have somewhat darker and more variable pixel brightness after color masking, and lesser surface area, was exploited for subsequent classification. Classification in all color spaces - red, green, and blue, and for both color masks, had an accuracy of nearly 80% (Table 2), well above the 50% level that would be expected from random chance. Hence, the technique was in accord with prior work using grayscale data, which lacked a preprocessing masking stage, and it likely can be useful to identify pathology in the videocapsule images. Moreover, if LDFs can be optimized, discrimination can be done not only automatically but in real time without *a priori* information, making it a potentially useful tool for analysis of incoming data as the capsule traverses the patient gastrointestinal tract. In future manifestations of the imaging systems available for videocapsule endoscopy, which might include a means to obtain biopsy samples, this technique could prove useful to identify regions of interest for biopsy sampling in real time as the capsule travels, without the need for guesswork.

Conflicts of interest

The authors have no conflicts of interest.

References

[1] A. Sapone, J.C. Bai, C. Ciacci, J. Dolinsek, P.H. Green, M. Hadjivassiliou, K. Kaukinen, K. Rostami, D.S. Sanders, M. Schumann, R. Ullrich, Spectrum of gluten-related disorders: consensus on new nomenclature and classification, BMC Med. 10 (2012) 13.
[2] A.R. Lee, D.L. Ng, J. Zivin, P.H. Green, Economic burden of a gluten-free diet, J. Hum. Nutr. Diet. 20 (2007) 423–430.
[3] P.H. Green, The many faces of celiac disease: clinical presentation of celiac disease in the adult population, Gastroenterology 128 (2005) S74–S78.
[4] J.W. Harper, S.F. Holleran, R. Ramakrishnan, G. Bhagat, P.H. Green, Anemia in celiac disease is multifactorial in etiology, Am. J. Hematol. 82 (2007) 996–1000.
[5] E.J. Ciaccio, S.K. Lewis, A.B. Biviano, V. Iyer, H. Garan, P.H. Green, Cardiovascular involvement in celiac disease, World J. Cardiol. 9 (2017) 652–666.
[6] S.H. Barton, D.G. Kelly, J.A. Murray, Nutritional deficiencies in celiac disease, Gastroenterol. Clin. N. Am. 36 (2007) 93–108.
[7] J.A. Abrams, B. Diamond, H. Rotterdam, P.H. Green, Seronegative celiac disease: increased prevalence with lesser degrees of villous atrophy, Dig. Dis. Sci. 49 (2004) 546–550.
[8] S.K. Lee, W. Lo, L. Memeo, H. Rotterdam, P.H. Green, Duodenal histology in patients with celiac disease after treatment with a gluten-free diet, Gastrointest. Endosc. 57 (2003) 187–191.
[9] B. Lebwohl, F. Granath, A. Ekbom, K.E. Smedby, J.A. Murray, A.I. Neugut, P.H. Green, J.F. Ludvigsson, Mucosal healing and risk for lymphoproliferative malignancy in celiac disease: a population-based cohort study, Ann. Intern. Med. 159 (2013) 169–175.
[10] A. Rubio-Tapia, M.W. Rahim, J.A. See, B.D. Lahr, T.T. Wu, J.A. Murray, Mucosal recovery and mortality in adults with celiac disease after treatment with a gluten-free diet, Am. J. Gastroenterol. 105 (2010) 1412–1420.
[11] P. Brar, S. Lee, S. Lewis, I. Egbuna, G. Bhagat, P.H. Green, Budesonide in the treatment of refractory celiac disease, Am. J. Gastroenterol. 102 (2007) 2265–2269.
[12] E.J. Ciaccio, C.A. Tennyson, G. Bhagat, S.K. Lewis, P.H. Green, Robust spectral analysis of videocapsule images acquired from celiac disease patients, Biomed. Eng. Online 10 (2011) 78.
[13] E.J. Ciaccio, C.A. Tennyson, G. Bhagat, S.K. Lewis, P.H. Green, Quantitative estimates of motility from videocapsule endoscopy are useful to discern celiac patients from controls, Dig. Dis. Sci. 57 (2012) 2936–2943.
[14] E.J. Ciaccio, C.A. Tennyson, G. Bhagat, S.K. Lewis, P.H. Green, Implementation of a polling protocol for predicting celiac disease in videocapsule analysis, World J. Gastrointest. Endosc. 5 (2013) 313–322.
[15] E.J. Ciaccio, C.A. Tennyson, G. Bhagat, S.K. Lewis, P.H. Green, Use of basis images for detection and classification of celiac disease, Bio Med. Mater. Eng. 24 (2014) 1913–1923.
[16] E.J. Ciaccio, G. Bhagat, S.K. Lewis, P.H. Green, Use of shape-from-shading to characterize mucosal topography in celiac disease videocapsule images, World J. Gastrointest. Endosc. 9 (2017) 310–318.
[17] E.J. Ciaccio, G. Bhagat, S.K. Lewis, P.H. Green, Extraction and processing of videocapsule data to detect and measure the presence of villous atrophy in celiac

disease patients, Comput. Biol. Med. 78 (2016) 97–106.
[18] S. Xavier, S. Monteiro, J. Magalhães, B. Rosa, M.J. Moreira, J. Cotter, Capsule endoscopy with PillCamSB2 versus PillCamSB3: has the improvement in technology resulted in a step forward? Rev. Esp. Enferm. Dig. 110 (2017) 155–159.
[19] S. Park, H.J. Chun, B. Keum, Y.S. Seo, Y.S. Kim, Y.T. Jeen, H.S. Lee, S.H. Um, C.D. Kim, H.S. Ryu, Capsule endoscopy to detect normally positioned duodenal papilla: performance comparison of SB and SB2, Gastroenterol. Res. Pract. 2012 (2012) 202935.
[20] S. Monteiro, F.D. de Castro, P.B. Carvalho, M.J. Moreira, B. Rosa, J. Cotter, PillCam® SB3 capsule: does the increased frame rate eliminate the risk of missing lesions? World J. Gastroenterol. 22 (2016) 3066–3068.
[21] M. Keuchel, N. Kurniawan, P. Baltes, D. Bandorski, A. Koulaouzidis, Quantitative measurements in capsule endoscopy, Comput. Biol. Med. 65 (2015) 333–347.
[22] G. Dimas, E. Spyrou, D.K. Iakovidis, A. Koulaouzidis, Intelligent visual localization of wireless capsule endoscopes enhanced by color information, Comput. Biol. Med. 89 (2017) 429–440.
[23] C. Spada, M.E. Riccioni, R. Urgesi, G. Costamagna, Capsule endoscopy in celiac disease, World J. Gastroenterol. 14 (2008) 4146–4151.
[24] T. Rokkas, Y. Niv, The role of video capsule endoscopy in the diagnosis of celiac disease: a meta-analysis, Eur. J. Gastroenterol. Hepatol. 24 (2012) 303–308.
[25] J.E.W. Koh, Y. Hagiwaraa, S.L. Oha, J.H. Tan, E.J. Ciaccio, P.H. Green, S.K. Lewisb, U.R. Acharya, Automated diagnosis of celiac disease using DWT and nonlinear features with video capsule endoscopy images, Future Generat. Comput. Syst. 90 (2019) 86–93.
[26] A. Klein, M. Gizbar, M.J. Bourke, G. Ahlenstiel, Validated computed cleansing score for video capsule endoscopy, Dig. Endosc. 28 (2016) 564–569.
[27] H.J. Song, J.S. Moon, K.N. Shim, Optimal bowel preparation for video capsule endoscopy, Gastroenterol. Res. Pract. 2016 (2016) 6802810.